RSC Advances

RSC Advances
Dynamic Article Links ►

Cite this: DOI: 10.1039/c0xx00000x

www.rsc.org/xxxxxx

ARTICLE TYPE

A novel porous substrate for the growth of high quality GaN crystals by HVPE

Yuanbin Dai[a], Yongzhong Wu[a], Lei Zhang[a], Yongliang Shao[a], Yuan Tian[a], Qin Huo[a], Peng Zhang[b], Xingzhong Cao[b], Xiaopeng Hao[a*]

An original high temperature annealing (HTA) technology has been established to fabricate a porous substrate with the layer of inverted pyramid structures. The details about the formation of the porous substrate and the related mechanism were discussed. It was proved that the porous structures were formed through an etching-like mechanism assisted by the SiO_2 patterned masks. High-quality GaN crystals have been prepared using the as-prepared porous substrate. The growth experiments demonstrated that such porous substrates were mechanically fragile. The porous structures are suitable to be used as a release layer for the growth of GaN crystals with low stress and defect density.

Introduction

GaN based III/V semiconductors are recognized as excellent materials for short-wavelength light emitting diodes (LEDs), laser diodes (LDs) and radio frequency power devices.[1-2] However, the optical and electrical properties of GaN-based devices are adversely affected by the mismatch caused by hetero-epitaxial growth on foreign substrates.[3] It is widely considered that the growth of GaN crystal with larger diameters is a possible solution. The hydride vapor phase epitaxy (HVPE) method, which is a promising method for the growth of large size GaN crystals in high-quality,[4] has been widely investigated. At present, HVPE is generally based on the crystallization of GaN on a foreign material,[5] where the large lattice and thermal expansion mismatch between GaN and foreign substrates leads to high residual stress. This results in a high density of threading dislocations and thus deteriorates both structural and electric properties of the grown crystal.[6]

A lot of attempts have been made to solve the problems mentioned above, one of the most promising approaches is the application of porous GaN buffer layer. Based on it, a technique known as void assisted separation (VAS) was obtained.[7-8] VAS technology was developed using the thin porous interlayer with nano-scale holes and numerous small voids between GaN layer and base substrate. The interlayer is important for the reduction of dislocation and the separation of GaN crystals without any cracks.

In this paper, a high temperature annealing (HTA) process assisted by the SiO_2 patterned masks was carried out to obtain a novel substrate bearing the layer of porous structures. To the best of our knowledge, this method has not been reported before. The features of this porous substrate were characterized. The details about the formation of the porous structures and the related mechanism were discussed. An attractive application of this porous templates is to grow GaN crystals by HVPE. Because the porous substrate retained the crystalline structure of the original MOCVD GaN, yet it was fragile and could be used as a buffer layer as well as the interlayer in VAS technology. The properties of the GaN crystals grown using this porous template by HVPE were studied by photoluminescence (PL), positron annihilation technology (PAT) and Raman spectra. The results showed that the porous structures were suitable to be used as a release layer for growth of GaN crystals with low stress and defect density.

a *State Key Lab of Crystal Materials, Shandong University, Jinan, 250100,China*
b Key Laboratory of Nuclear Analysis Techniques, Institute of High Energy Physics, Chinese Academy of Sciences, Beijing 100049, China
**. E-mail: xphao@sdu.edu.cn;*
Fax: +8653188364864; Tel: +8653188366218

Experimental

2-5 μm GaN layer was grown on a 2-inch c-plane sapphire substrate by metal-organic chemical vapor deposition (MOCVD-GaN). The dislocation density of the MOCVD-GaN is about $10^8 cm^{-2}$. Then the SiO_2 layer was deposited by plasma-enhanced chemical vapor deposition and processed into a square arrangement masks structure by conventional photolithography and wet etching technology. Then, the patterned masks GaN sample was heated to approximately 1100°C in a N_2 atmosphere at atmospheric pressure. The sample was annealed for several hours and cooled down. After cleaning, the sample with porous structures was employed as the substrate of GaN crystals growth by HVPE. The annealing and the subsequent GaN crystals growth were both carried out in a vertical HVPE reactor.[9-10]

In order to characterize the optical properties, PL measurements were carried out at room temperature using a 325 nm He-Cd laser as the excitation source. The surface morphology was confirmed by scanning electron microscopy (SEM, Hitachi S4800). PAT is a useful technique for vacancy-type defects investigation. Slow positron beam Doppler broadening of annihilation radiation was performed to obtain information on native vacancies in GaN crystals. Raman spectra were carried out on a Horiba Jobin Yvon LabRAM HR system at room temperature using a 532 nm solid state laser as the excitation source.

Results and discussion

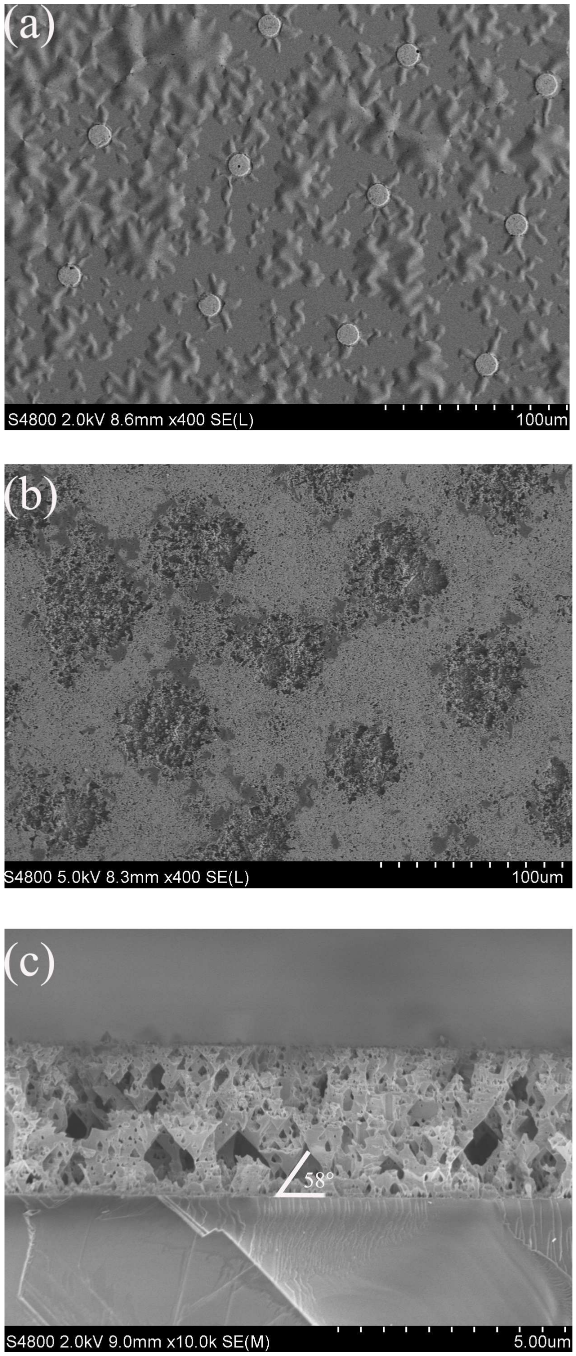

Fig. 1 SEM images of the porous substrate (a) top view of the sample after being annealed (b-d) surface of the sample after ultrasonic process (e-f) sectional view of the porous sample after being cleaned

A top view of the sample after being annealed for 2h is shown in Fig 1(a). It can be seen that the peeling SiO_2 layer results in a peeling area ratio about 50-60%. Then the sample with a peeling SiO_2 layer was cleaned though a 10 min ultrasonic process in H_3PO_4. The area near the opening of the mask was annealed to a pit with bigger diameter than the pattern as shown in Fig 1(b). Some discernible hexagonal pits were also formed on the remaining surface. And then, the residual SiO_2 mask was removed by hydrofluoric acid. A cross-sectional SEM image of the porous sample is shown in Fig 1(c). The layer of inverted pyramid porous structures can be seen clearly. And the porous structures distributed throughout the lateral extensive area. There is a dependence on the crystallographic orientation at most angles of 58° with the c-plane defined by the $(\bar{1}\bar{1}2\bar{2})$ plane.

The inverted pyramid shape is similar to the chemical etching studies of c-plane GaN. Gao et al. [11] reported that a photo-electrochemical wet etching on GaN was correlative to the polarity and dislocation. Smooth etched surfaces were formed with the $(\bar{1}\bar{1}2\bar{2})$ facet as an etch stop plane. Lo et al. [12] found that the inverted pyramid structure was created at the GaN-sapphire interface by anisotropic chemical wet etching. Qi et al. [13] found that more facets and varied inclination of the facet appeared by H_3PO_4 etching, while only the crystallographic $(10\bar{1}\bar{1})$ facets were obtained by KOH etching.

Under higher magnification of the porous sample, it can be observed that the decomposition was selective for the inverted pyramid porous structures formation. These planes after annealing have also been the predominant GaN faces appeared in etching study mentioned above. And the density of the inverted pyramid structures was different between the area near the N-face and Ga-face of the GaN. We considered that it was sensitive to polarity thermodynamics from which the activation energy of Ga-face is much bigger than that of N-face GaN.[13] The annealing process results are consistent with the etching studies. All results suggest that the mechanism of the thermally activated porous formation by the high temperature annealing technology is similar to the etching which is dislocation-mediated process.

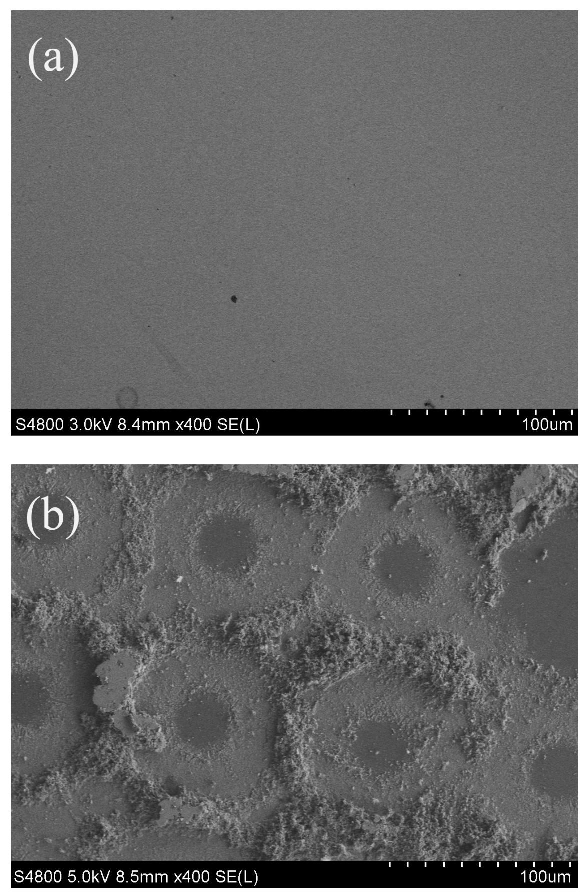

Fig.2 SEM images of samples (a) with a complete SiO_2 and (b) with the patterned masks after being annealed for 4h

Fig 2(a) shows the top view SEM image of the sample with a complete un-patterned SiO_2 layer after the same annealing that process of 4h. After removing the SiO_2 layer, It is observed GaN was not decomposed and the underlying GaN was completely protected. This proved that the SiO_2 mask protected the underlying GaN from decomposition. Fig 2(b) shows the top view of the samples with the patterned SiO_2 layer after the same annealing process of 4 hours. After cleaning, it is observed that the honeycomb structures of GaN are left. The area of the adjacent openings decomposed totally. It is clear that the decomposition turned into the lateral direction continuously.

Based on the above observations, after the annealing process the porous structures are formed through an etching-like mechanism[6], we suggest, considering the assisting effect of the SiO_2 patterned masks as illustrated in Fig 3. At first a layer of SiO_2 masks is fabricated with a designed thickness and pattern as shown in Fig 3(a). When the sample is heated to the annealing temperature, the GaN begins to decompose which has been reported as follows.[14]

$$GaN(s) \rightarrow Ga(g) + (1-i)N + 0.5iN_2 \qquad (1)$$

The decomposition is selective for the dislocation as shown in Fig 3(b) explained by Cabrera's thermodynamic theory. The activation energy at a dislocation site is:

$$\Delta G_d^* \cong \Delta G_p^* \sqrt{1 - 4\frac{r_F}{r_c}} \qquad (2)$$

Where $r_F = Gb^2\alpha / 8\pi^2\gamma$ represents the Frank's radius, ΔG_p^* is the activation energy at a perfect surface which can be expressed as

$$\Delta G_P^* = \pi h \gamma r_c \qquad (3)$$

G is the shear modulus, b is the Burgers vector of dislocation, r is the radius of the dislocation and α is related to the type of different material dislocation. According to the Equation 2-3, the decomposition is favoured at a dislocation site because ΔG_d^* is always smaller than ΔG_p^*.[15]

The subsequent annealing is a dislocation-mediated process by the SiO_2 patterned masks assisted. With the process of decomposition, the flowing N_2 takes the Ga vapor away from the GaN surface momentarily. Inside the GaN, the gallium vapor turns to liquid in a short time because of the high boiling point of Ga (2403℃). Schoonmaker et al.[16] found that liquid Ga may participate as a catalyst in the vaporization process by dissolving Ga and disrupting its rigid wurtzite crystal structure. So decomposition of the inside GaN continues downward and turns laterally to form channels through the adjacent opening by the catalytic effect of liquid gallium as shown in Fig 3(c). During annealing treatment, the vapour may diffuse to the gap between the SiO_2 layer and the underlying GaN as a result of the thermal mismatch. A peeling SiO_2 layer is formed on the surface as shown in Fig 3(d). The decomposition is thermally activated. The rate is strongly dependent on the crystalline quality of the GaN. The presence of dislocations can locally influence the activation energy of the GaN available for the decomposition reaction rate. So the decomposition is perfectly selective to obtain a large number of inverted pyramid porous structures. And there is some crystallographic orientation dependence which is believed to be the ($\bar{1}\bar{1}2\bar{2}$) plane. The ($\bar{1}\bar{1}2\bar{2}$) plane is the more chemically inert plane as an etch-stop plane.[17] Higher porosity of GaN layer is created at interface between GaN and sapphire because the dislocation density is larger. When cooling down, there is always liquid Ga left. It is cleaned by an ultrasonic process in H_3PO_4.

The patterned masks are important for the formation of porous structures. We also used a GaN sample without a SiO_2 layer in the same annealing process for comparison, it exhibited only a roughened surface with hills and pits. Delicately adjusting the annealing condition, porous structure might also be possible which is now under investigation.[18] We supposed that the formation of porous structures is sensitive to the ratio between the lateral decomposition rate and vertical decomposition rate[13]. The lateral rate relies more on kinetic factors and the vertical rate relies more on thermodynamic factors such as the temperature and surface energy. At the opening area, the vertical rate is far larger than the lateral rate. So the opening area was

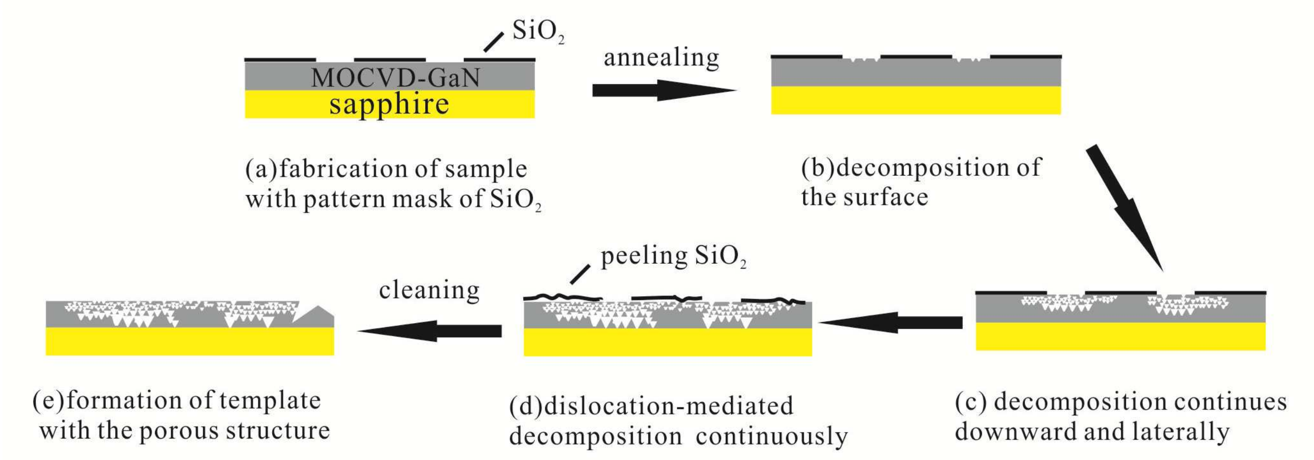

Fig. 3 Schematic of the porous substrate formation by the HTA process

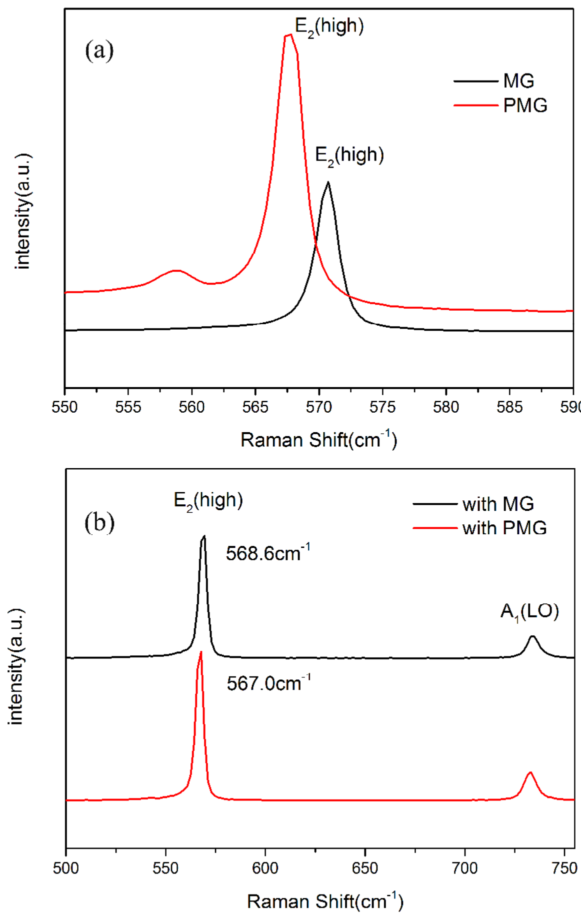

Fig.4 Raman spectra of (a) the MG and PMG substrate and (b) GaN crystals grown on the MG and PMG by HVPE

decomposed to pits as shown in Fig 1(b). The area protected by the masks has a larger lateral rate catalyzed by liquid Ga. In this condition the surface is flat with porous structures underneath as shown in Fig 1(b, c).

Fig. 4(a) is the Raman spectra of porous MOCVD-GaN substrate (PMG) obtained by the HTA technology and MOCVD-GaN substrate (MG) before annealing. The E_2 (high) phonon mode is used in the characterization of the strain state in GaN crystals by the following equation[19-20].

$$\sigma = \frac{\Delta\omega}{4.3}(\mathrm{cm}^{-1} GPa^{-1}) \qquad (4)$$

Where σ is the biaxial stress and Δω is the E_2 phonon mode peak shift. The E_2 (high) mode peak position of stress-free GaN is believed to be 566.2cm^{-1}.[21] It can be observed that the stress is significantly lower for PMG than that of MG. Such PMG appeared mechanically fragile to be used as a release layer.[22] We employed the PMG as buffer layer to fabricate the GaN by HVPE. To make comparisons, a reference wafer of MG also went through exactly the same fabrication process.

Fig. 4(b) shows the Raman spectra of GaN crystals grown on the MG and PMG by HVPE. The E_2(high) phonon mode peak positions for GaN crystals grown on MG and PMG were located at 568.6cm^{-1} and 567.0cm^{-1} as shown in Fig 7. According to the Eq.4, it can be calculated that the compressive stress existing in the HVPE GaN crystals grown on the MG and the PMG was approximately 0.558 GPa and 0.186 GPa, respectively. The results indicate that the residual stress in the HVPE GaN crystals grown on the PMG was reduced. The porous substrate is beneficial to the release of residual stress.

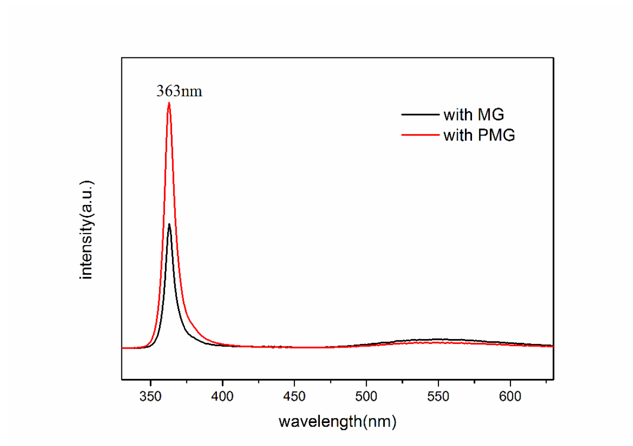

Fig. 5 PL spectra of GaN crystals grown on MG and PMG

The optical properties of the HVPE GaN crystals grown on MG and PMG were investigated by room temperature PL spectroscopy. Band-edge emission peaks at 363nm of HVPE GaN crystals grown on MG and PMG are observed in Fig.5. The FWHM of the peaks is narrow as a result of the high quality of the HVPE GaN crystals. The shift of the peaks can be associated with the relaxation of stress. The band edge emission intensity of the GaN crystals grown on the PMG by HVPE is higher than that for the MG. There is a small yellow luminescence band at 500–600 nm. The intensity of the yellow luminescence peak of the GaN crystals grown on the PMG by HVPE is lower than that of the MG.

The positron annihilation technology was used to obtain information of native vacancies in GaN. Positrons get trapped at neutral and negative vacancies because of the missing positive charge of the ion cores. The GaN crystals grown on the PMG by HVPE were investigated with slow positron beam Doppler broadening experiments at room temperature described using the conventional low and high electron-momentum parameters S and W.

Fig. 6(a) is the electron-momentum parameters S and W in the HVPE GaN crystals .The data in all HVPE GaN crystals forms a straight line in the (S, W) plane indicating that the same defect (Ga vacancy) is found in all samples.[23] When positrons annihilate at vacancies, the S parameter increases and the W parameter decreases, because a larger fraction of annihilations takes place with the valence electrons with lower momentum. Consequently, the lower S parameter, the lower concentration of vacancies[24].

The S parameter measured as a function of positron implantation energy is shown in Fig. 6(b). The positron implantation energy means implantation depth which can be determined with the simple formula:

$$R = \left(\frac{40}{\rho}\right) E^{1.6} \qquad (5)$$

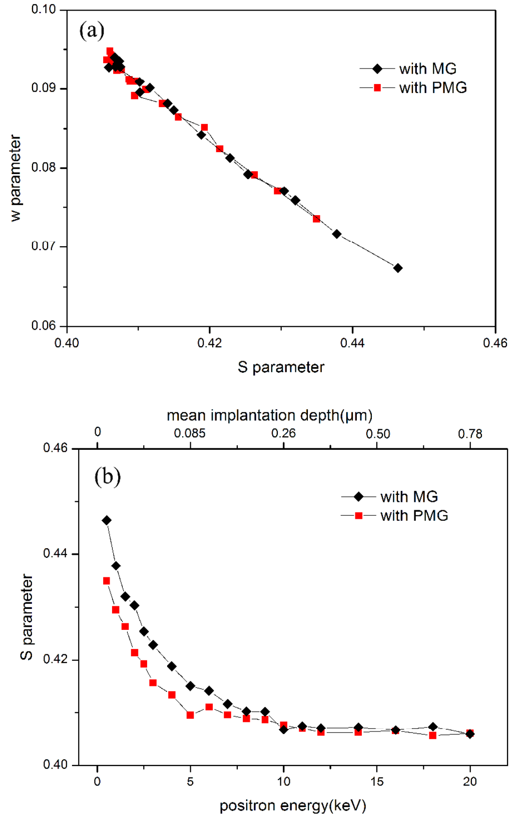

Fig. 6 (a) Electron-momentum parameters S and W in the GaN crystals grown on MG and PMG (b) S parameter measured as a function of the positron incident energy for GaN crystals grown on MG and PMG

Where R is the implantation depth (nm), ρ is the GaN density (g/cm^3), E is the positron implantation energy (keV).

The S parameters were constant for high energy (>10kev) indicating that all positrons annihilate in the crystals at the depth of 0.25μm[25]. For low energy positrons(0-10 keV) implanted close to the crystal surface, the S parameters were 0.41-0.45 characteristic for the Ga vacancy of the near-surface region of the crystal at the depth of 0-0.25 μm. It is observed that the S parameter for crystal grown on PMG by HVPE was lower than that for MG in Fig 6(b). It indicated that the concentration of vacancies in HVPE GaN crystals grown on MG was higher than that of GaN grown on PMG. This is in line with the result of yellow luminescence. The Ga vacancy concentration correlates with the intensity of the yellow luminescence, suggesting that the acceptor states of V_{Ga} are involved in this optical transition.[25]

Conclusion

In conclusion, we have investigated the structure of the porous layer obtained by HTA technology. It was shown that the mechanism of the thermally activated porous structures formed by the high temperature annealing technology is dislocation-mediated. The patterned masks are important for the formation of porous structures by adjusting the ratio between the lateral decomposition rate and vertical decomposition rate. The porous MOCVD GaN layer was characterized by a lower level of residual stresses than the epitaxial MOCVD GaN layer. Utilizing the as-prepared porous substrate as buffer layer, GaN crystals with low stress and defect densities were obtained by HVPE. The porous substrate was beneficial to the release of residual stress. According to the optical property of the GaN crystals, it was concluded that the porous substrate increased the intensity of GaN crystal band-edge emission. The Ga vacancy concentration correlated with the intensity of the yellow luminescence, suggesting that the acceptor states of V_{Ga} were involved in this optical transition. The results showed the feasibility of proposed novel method for the fabrication of high quality GaN crystals.

Acknowledgements

This work was supported by National Basic Research Program of China (2011CB301904), NSFC (Contract No. 51321091) and IIFSDU.

1. S. Nakamura, T. Mukai and M. Senoh, *Applied Physics Letters*, 1994, **64**, 1687.
2. S. Nakamura, M. Senoh, S.-i. Nagahama, N. Iwasa, T. Yamada, T. Matsushita, H. Kiyoku and Y. Sugimoto, *Japanese Journal of Applied Physics Part 2 Letters*, 1996, **35**, L74-L76.
3. Y. Fu, Y. T. Moon, F. Yun, U. Ozgur, J. Q. Xie, S. Dogan, H. Morkoc, C. K. Inoki, T. S. Kuan, L. Zhou and D. J. Smith, *Applied Physics Letters*, 2005, **86**, 043108.
4. C. Hennig, E. Richter, M. Weyers and G. Tränkle, *Journal of Crystal Growth*, 2008, **310**, 911-915.
5. M. Amilusik, T. Sochacki, B. Łucznik, M. Boćkowski, B. Sadovyi, A. Presz, I. Dzięcielewski and I. Grzegory, *Journal of Crystal Growth*, 2013, **380**, 99-105.
6. M. Mynbaeva, A. Titkov, A. Kryganovskii, V. Ratnikov, K. Mynbaev, H. Huhtinen, R. Laiho and V. Dmitriev, *Applied Physics Letters*, 2000, **76**, 1113-1115.
7. Y. Oshima, T. Eri, M. Shibata, H. Sunakawa and A. Usui, *physica status solidi (a)*, 2002, **194**, 554-558.
8. T. Yoshida, Y. Oshima, T. Eri, K. Ikeda, S. Yamamoto, K. Watanabe, M. Shibata and T. Mishima, *Journal of Crystal Growth*, 2008, **310**, 5-7.
9. L. Zhang, Y. L. Shao, X. P. Hao, Y. Z. Wu, H. D. Zhang, S. Qu, X. F. Chen and X. G. Xu, *Crystengcomm*, 2011, **13**, 5001-5004.
10. H. Zhang, Y. Shao, L. Zhang, X. Hao, Y. Wu, X. Liu, Y. Dai and Y. Tian, *Crystengcomm*, 2012, **14**, 4777-4780.
11. Y. Gao, M. D. Craven, J. S. Speck, S. P. Den Baars and E. L. Hu, *Applied Physics Letters*, 2004, **84**, 3322-3324.
12. M. H. Lo, P. M. Tu, C. H. Wang, C. W. Hung, S. C. Hsu, Y. J. Cheng, H. C. Kuo, H. W. Zan, S. C. Wang, C. Y. Chang and S. C. Huang, *Applied Physics Letters*, 2009, **95**, -.
13. S. L. Qi, Z. Z. Chen, H. Fang, Y. J. Sun, L. W. Sang, X. L. Yang, L. B. Zhao, P. F. Tian, J. J. Deng, Y. B. Tao, T. J. Yu, Z. X. Qin and G. Y. Zhang, *Applied Physics Letters*, 2009, **95**, -.
14. B. V. L'vov, *Thermochimica Acta*, 2000, **360**, 85-91.
15. Y. Tian, Y. Wu, Y. Shao, Y. Dai, H. Zhang, R. Wei and X. Hao, *CrystEngComm*, 2014.
16. R. C. Schoonmaker, A. Buhl and J. Lemley, *The Journal of Physical Chemistry*, 1965, **69**, 3455-3460.
17. H.-H. Huang, H.-Y. Zeng, C.-L. Lee, S.-C. Lee and W.-I. Lee, *Applied Physics Letters*, 2006, **89**, -.
18. C. Miao, Y. Honda, M. Yamaguchi and H. Amano, *Japanese Journal of Applied Physics*, 2013, **52**, 08JB03.
19. V. Y. Davydov, N. S. Averkiev, I. N. Goncharuk, D. K. Nelson, I. P. Nikitina, A. S. Polkovnikov, A. N. Smirnov, M. A. Jacobson and O. K. Semchinova, *Journal of Applied Physics*, 1997, **82**, 5097-5102.
20. H. Hartono, C. B. Soh, S. Y. Chow, S. J. Chua and E. A. Fitzgerald, *Applied Physics Letters*, 2007, **90**, -.

21. C. Kisielowski, J. Krüger, S. Ruvimov, T. Suski, J. Ager III, E. Jones, Z. Liliental-Weber, M. Rubin, E. Weber and M. Bremser, *Physical Review B*, 1996, **54**, 17745.
22. S. Huang, Y. Zhang, B. Leung, G. Yuan, G. Wang, H. Jiang, Y. Fan, Q. Sun, J. Wang, K. Xu and J. Han, *ACS Applied Materials & Interfaces*, 2013, **5**, 11074-11079.
23. G. Koblmuller, F. Reurings, F. Tuomisto and J. Speck, *Applied Physics Letters*, 2010, **97**, 191915-191915-191913.
24. K. Saarinen, T. Laine, S. Kuisma, J. Nissilä, P. Hautojärvi, L. Dobrzynski, J. M. Baranowski, K. Pakula, R. Stepniewski, M. Wojdak, A. Wysmolek, T. Suski, M. Leszczynski, I. Grzegory and S. Porowski, *Phys Rev Lett*, 1997, **79**, 3030-3033.
25. K. Saarinen, P. Seppala, J. Oila, P. Hautojarvi, C. Corbel, O. Briot and R. L. Aulombard, *Applied Physics Letters*, 1998, **73**, 3253-3255.

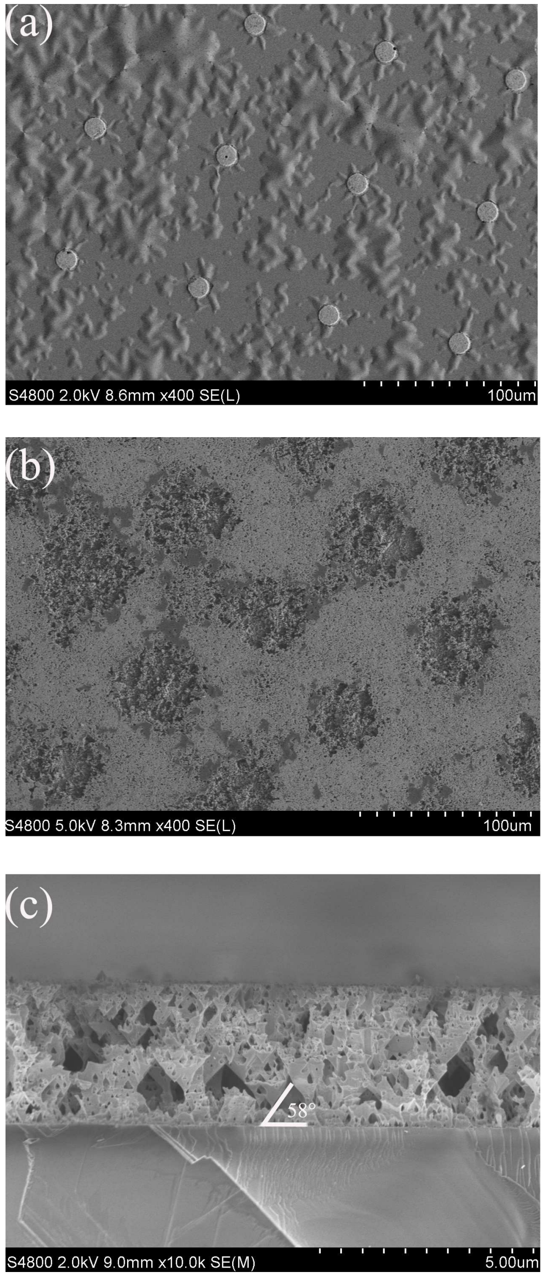

Fig. 1 SEM images of the porous substrate (a) top view of the sample after being annealed (b-d) surface of the sample after ultrasonic process (e-f) sectional view of the porous sample after being cleaned

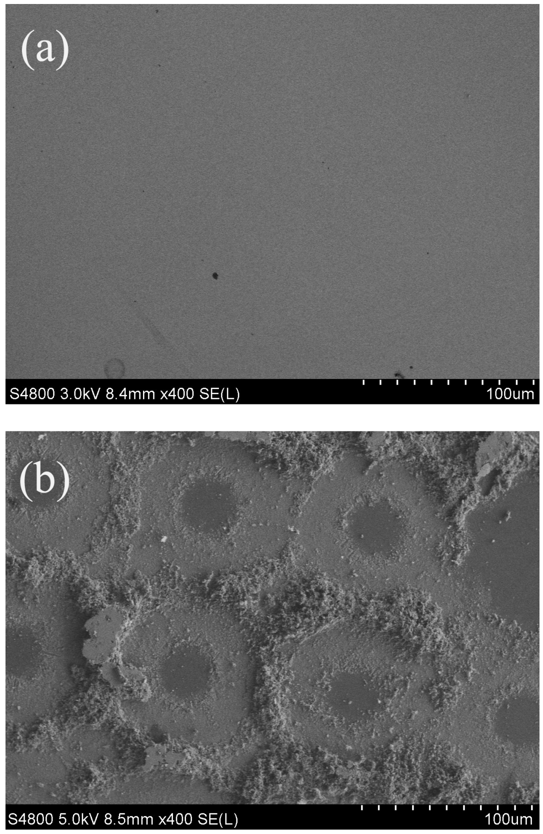

Fig.2 SEM images of samples (a) with a complete SiO_2 and (b) with the patterned masks after being annealed for 4h

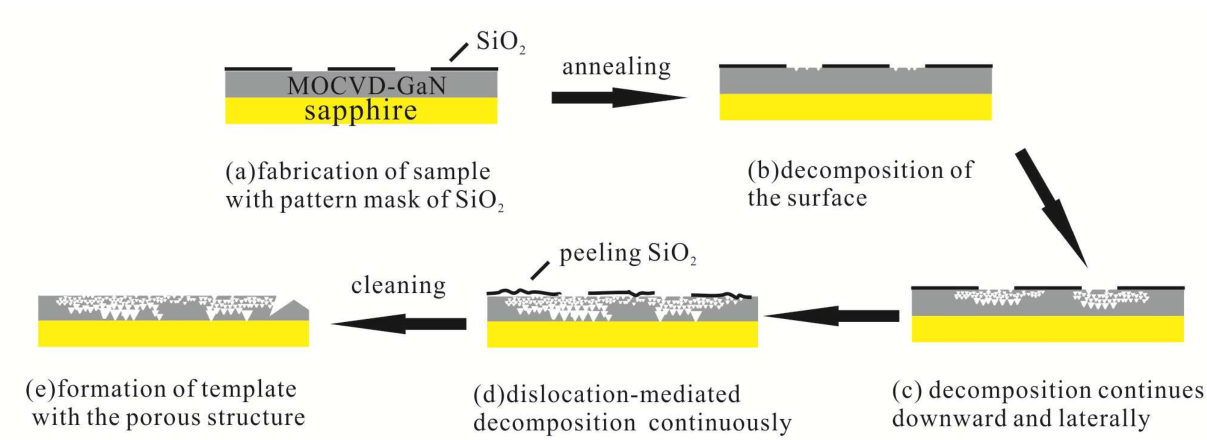

Fig. 3 Schematic of the porous substrate formation by the HTA process

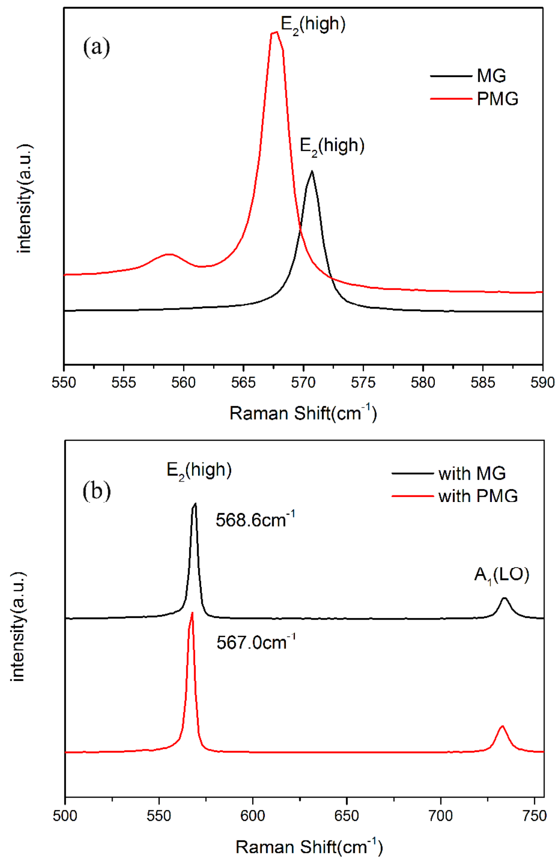

Fig.4 Raman spectra of (a) the MG and PMG substrate and (b) GaN crystals grown on the MG and PMG by HVPE

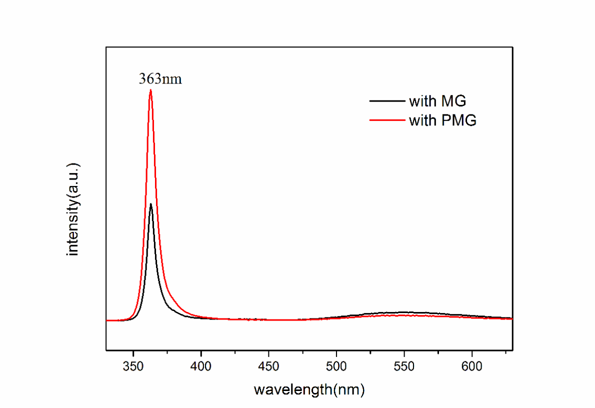

Fig. 5 PL spectra of GaN crystals grown on MG and PMG

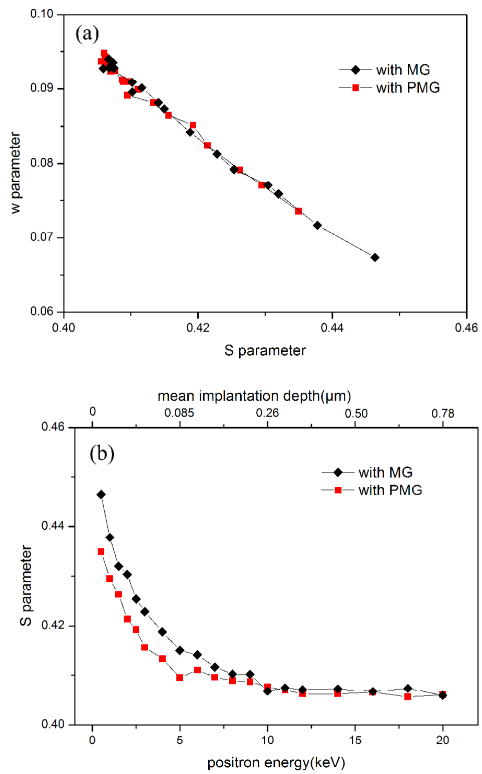

Fig. 6 (a) Electron-momentum parameters S and W in the GaN crystals grown on MG and PMG (b) S parameter measured as a function of the positron incident energy for GaN crystals grown on MG and PMG

A novel porous substrate for the growth of high quality GaN crystals by HVPE

Yuanbin Dai[a], Yongzhong Wu[a], Lei Zhang[a], Yongliang Shao[a], Yuan Tian[a], Qin Huo[a], Peng Zhang[b], Xingzhong Cao[b], Xiaopeng Hao[a*]

An original high temperature annealing (HTA) technology has been established to fabricate a porous substrate with the layer of inverted pyramid structures. The details about the formation of the porous substrate and the related mechanism were discussed. It was proved that the porous structures were formed through an etching-like mechanism assisted by the SiO_2 patterned masks. High-quality GaN crystals have been prepared using the as-prepared porous substrate. The growth experiments demonstrated that such porous substrates were mechanically fragile. The porous structures are suitable to be used as a release layer for the growth of GaN crystals with low stress and defect density.